"Revision 2 corrected"
Influence of hydration on ^{23}Na, ^{27}Al and ^{29}Si MAS-NMR spectra of sodium saponites and sodium micas

J. Sanz[#], I.Sobrados[#] and J. L. Robert*

[#] Instituto de Ciencia de Materiales de Madrid, CSIC, Cantoblanco, 28049 Madrid, Spain

*IMPMC, UMR 7590, CNRS-Université Pierre et Marie Curie, Case courrier 115, 4 place Jussieu, 75252 Paris Cedex 05, France

Corresponding author : jsanz@icmm.csic.es

Abstract

Synthetic sodium saponites, $Na_xMg_3(Si_{4-x}Al_x)O_{10}(OH)_2.nH_2O$, with $0.33 \leq x \leq 1$, and trioctahedral Na-micas series, $Na(Mg_{3-y}Al_y)(Si_{3-y}Al_{1+y})O_{10}(OH)_2.nH_2O$, with $0 \leq y \leq 1$, have been investigated by MAS-NMR spectroscopy. The presence of anhydrous, mono- and two-layers hydrates, deduced by X-ray diffraction, has been associated with specific lines detected in ^{23}Na MAS-NMR spectra. In these phyllosilicates, the location of tetra- and octahedral charge has been analyzed by ^{27}Al MAS-NMR spectroscopy. The salient result is the major effect of the interlayer charge on ^{29}Si chemical shift of the four NMR components ascribed to Si_3, Si_2Al, $SiAl_2$ and Al_3 environments. This effect is much more important than the most commonly accepted contribution of the ditrigonal distortion of tetrahedral sheets. In saponites, ^{29}Si MAS-NMR spectra change considerably with the sodium hydration. In dehydrated samples, where Na cations are engaged in two pseudo-hexagonal cavities, ^{29}Si MAS-NMR components split as a consequence of the partial sodium occupancy of three neighbouring hexagonal rings that surrounds a particular tetrahedron. In hydrated samples, where Na^+ cations interact with water, chemical shifts of resolved components are averaged as a consequence of interlayer water and cation mobilities.

Key-words: 2:1 phyllosilicates, ^{29}Si, ^{27}Al and ^{23}Na MAS-NMR spectroscopy, Si-Al distribution, charge location, hydration state.

INTRODUCTION

In trioctahedral 2:1 Na-phyllosilicates $Na_{0-1}M_3T_4O_{10}(OH)_2$, where M stands for Mg, Al and T for Si, Al; tetrahedra T share three oxygens with neighbouring tetrahedra to form hexagonal rings (Figure 1). In these silicates, charge deficits introduced by the substitution of $^{[4]}Si^{4+}$ by $^{[4]}Al^{3+}$ are compensated by the incorporation of interlamellar Na^+ cations in saponites $Na_xMg_3(Si_{4-x}Al_x)O_{10}(OH)_2.nH_2O$ or by the substitution of Mg^{2+} by Al^{3+} in the octahedral sheet of micas $Na(Mg_{3-y}Al_y)(Si_{3-y}Al_{1+y})O_{10}(OH)_2.nH_2O$.

In phyllosilicates 2:1, Al for Si substitution increases the tetrahedral layer dimensions making difficult the matching of the octahedral with two tetrahedral layers. This dimensional misfit is compensated by the opposite rotation of adjacent tetrahedra by an angle α around the c* direction (Figure 1), and by the flattening of octahedra into trigonal antiprisms (Bailey, 1984, Sanz and Robert, 1992). From this fact, the size of the interlamellar cations can limit the tetrahedral distortion in anhydrous phases (Bailey,1984; for a compilation). In hydrated samples, single and double-layer phases, with basal spacings near 12 and 15 Å, are the most frequent hydration states of Na-phyllosilicates (Carman, 1974; de la Calle and Suquet, 1988; Güven, 1988). In these phases, the arrangement of water and sodium cations changes appreciably with the hydration state.

NMR spectroscopy has been extensively used to study the tetrahedral framework of phyllosilicates 2:1 (Sanz and Serratosa, 1984, Sanz and Robert, 1992). The detection of tetra- and octahedral Al components in ^{27}Al MAS-NMR spectra make possible the analysis of substitutional schemes in phyllosilicates. On the other hand, it was shown that ^{29}Si MAS-NMR chemical shifts associated with Si in $Si_{3-n}Al_n$ environments (n =0, 1, 2 and 3) depend on the interlayer charge, playing a secondary role the octahedral one (Sanz et al., 2006a). Some characteristics of

the Si,Al distribution have been previously deduced from the analysis of the relative intensities of $Si_{3-n}Al_n$ components. In particular, it was shown that the distribution of Si and Al complies besides the Loewenstein's rule (Al_t-O-Al_t avoidance), with the homogeneous dispersion of charges (HDC) model, proposed by Herrero et al. (1985) and Circone et al. (1991). In this model, the number of Al per hexagonal ring was assumed to be as close as possible to the mean value deduced from structural formulae.

Finally, hydration states deduced by X-ray diffraction (Figure 2) can be correlated with information obtained by ^{23}Na NMR spectroscopy, as anhydrous, mono- and two-layer hydrates give specific lines at different chemical shift values (Laperche et al., 1990). In two layer hydrates, the analysis of ^{1}H NMR spectra afforded information about interactions of water with compensating cations and tetrahedral layers (Hougardy et al., 1970 and 1976). In one-layer hydrated Na-micas, contiguous layers are shifted relative to each other, favouring a stronger interaction of hydrated sodium cations, $Na.2H_2O$, with four tetrahedra of two contiguous layers (de la Calle and Suquet, 1988; Sanz et al., 2006b). In anhydrous micas, Na^+ ions are engaged in two hexagonal rings of contiguous layers, interacting with oxygens of eight tetrahedra (Rausell-Colom et al., 1980, Kogure et al., 2004, 2005).

In the present work, we have analyzed synthetic Na-saponites and Na-micas by ^{29}Si, ^{27}Al and ^{23}Na MAS-NMR spectroscopy. In particular, the influence of interlayer charge on chemical shifts of NMR components will be first investigated. In the second stage, the effect of interlamellar water will be discussed by comparing NMR spectra of hydrated and dried samples.

EXPERIMENTAL

Materials

All layer silicates investigated in the present study were obtained by hydrothermal synthesis using silicate gels as starting compounds. The gels were prepared

according to a method derived from that of Hamilton and Henderson (1968), using high grade reagents: dried Na_2CO_3, titrated solutions of Mg and Al nitrates, and tetraethylorthosilicate TEOS, $(C_2H_5O)_4Si$, as silica source. Saponites were synthesized in Morey-type pressure vessels, internally coated by a silver tube, at 400ºC, 1 kbar PH_2O, for a run duration of 4 weeks. Micas were synthesized in Tuttle-type pressure vessels, in sealed gold tubes, at 600ºC, 1 kbar PH_2O, for run durations of 2 weeks. In both cases, the uncertainties on temperature and pressure are ± 10ºC and ± 50 bars, respectively. Chemical compositions of samples were deduced with Inductively Coupled Plasma (ICP) technique. Deduced compositions were near nominal compositions; Sanz and Robert (1992) (Table 1).

In saponites $Na_xMg_3(Si_{4-x}Al_x)O_{10}(OH)_2.nH_2O$, with $0.33 \leq x \leq 1$, the incorporation of Al in the tetrahedral sheet is compensated by interlamellar sodium. In these phyllosilicates, the dominant hydration state is the “two-layer” one (n = 5), but the “one-layer” form (n = 2) can also be formed. Dehydration of saponites produced anhydrous single phases.

Na-micas, $Na(Mg_{3-y}Al_y)(Si_{3-y}Al_{1+y})O_{10}(OH)_2.nH_2O$, belong to the Na- phlogopite - preiswerkite join, where y is the rate of the so-called “Al-Tschermak“ substitution, with $0 \leq y \leq 1$.

$$^{[6]}Mg^{2+}, {}^{[4]}Si^{4+} \Leftrightarrow {}^{[6]}Al^{3+}, {}^{[4]}Al^{3+}.$$

In micas, the deficit of tetrahedral charge introduced by Al is mainly compensated by substitution of Mg^{2+} by Al^{3+} in the octahedral sheet. The Na-phlogopite, i.e. aspidolite, $NaMg_3(Si_3Al)O_{10}(OH)_2.nH_2O$, corresponds to y = 0 (Rieder et al., 1999), and preiswerkite, $Na(Mg_2Al)(Si_2Al_2)O_{10}(OH)_2$, to y = 1 (Oberti et al., 1993). For $0 \leq y \leq 0.75$, Na-micas are hydrated, the “one-layer” hydrate (n = 2) being dominant; however, for $y > 0.75$ only anhydrous phases are stabilized (Liu, 1989). Dehydration of hydrated micas produced anhydrous single phases.

In saponites, interlamellar Na cations compensate charge deficits created by tetrahedral Al; however, in micas the excess of charge created by octahedral Al is compensated by charge deficits produced by tetrahedral Al. The preparation of samples without paramagnetic cations preserves NMR resolution. In this work, information deduced from ^{27}Al and ^{29}Si MAS-NMR spectra will be used to investigate the location of charge deficits in phyllosilicates. In the following, saponite and mica tetrahedral compositions are given in terms of the tetrahedral Al fractional content $x_t = Al_t/(Al_t + Si)$, with $0 \leq x_t \leq 0.5$.

Methods

XRD patterns were recorded with a Siemens diffractometer ($\theta/2\theta$ Bragg-Brentano geometry), working at 40 kV and 40 mA. XRD patterns were recorded under controlled humidity conditions (P/P_0= 85%) in the 20-120º 2θ range, using the CoKα Fe filtered radiation (λ = 1.7902 Å), with the step-scanning mode (0.02º step) and 8s of counting time per step. For d spacing measurements, high-grade powdered Si was used as internal standard.

^{29}Si, ^{27}Al and ^{23}Na NMR spectra were recorded at 79.5, 104.3 and 105.8 MHz with a Bruker MSL-400 spectrometer. The external magnetic field was 9.4 Tesla. Dehydration of Na-saponites and Na-micas was achieved by heating samples at 200ºC for 12 hours, in a glove box swept by a dry nitrogen stream. The sample holder was filled up within the glove box, and sealed with wax to prevent the possible rehydration of the sample during spectra acquisition. The MAS-NMR experiments were performed at room temperature in samples spun around the magic angle (54º 44' with respect to the magnetic field) at 4-4.5 kHz in the case of ^{29}Si and 10 kHz for ^{27}Al and ^{23}Na signals. The NMR spectra were recorded after $\pi/2$ and $\pi/8$ pulse excitations of Si and Al (or Na) signals (4 and 2 μsec). The interval between successive accumulations (6-10 s) was chosen to avoid saturation effects. TMS and 1M solutions of $AlCl_3$ and NaCl were used as external standards for ^{29}Si, ^{27}Al and ^{23}Na NMR signals. In the case of Al MAS-NMR spectra, the presence of second order quadrupole effects makes

difficult the determination of chemical shift values. Errors in band positions are lower than 0.2 ppm.

To preserve quantitative analyses, no mathematical procedure of NMR signal treatment, such as multiplication by an exponential function, was used. Analysis of MAS-NMR spectra was carried out using the Bruker program WINFIT (Massiot, 1993). Deconvolution used a standard non linear least squares fitting method. The spinning rate and position, linewidth and intensity of components were automatically determined. When resolution of NMR components was poor, linewidths of components were constrained to vary together. In quantitative analysis of spectra, relative intensities of components were determined by numerical integration. In Al MAS-NMR spectra, the presence of second order quadrupolar effects makes difficult the analysis of spinning sideband patterns; and from that, the precise determination of relative intensity of tetra and octahedral Al components. Errors in determination of relative band intensities of central components are lower than 5 %.

RESULTS

The XRD technique has been used to analyze the nature of hydrate phases in phyllosilicates. In each phase, the ditrigonal rotation angle (α) has been determined from XRD data using the model of Donnay et al. (1964 a and b), which correlates the α-angle with the cell parameter b and the average T-O distance, d_t, in tetrahedra (Figure 1):

$$\cos \alpha = b/4.\sqrt{2}.d_t.$$

The average T-O distance, d_t, was calculated using the relation of Hazen and Burnham (1973):

$$d_t = 0.163\ ^{[4]}(Al/Al + Si) + 1.608\ Å.$$

This method reproduces α values, deduced from single crystal measurements, within a precision of ± 1º. Table 1 includes composition, d_t and α values of phyllosilicates analyzed in this work.

^{23}Na MAS-NMR spectra of hydrated phyllosilicates are given in Figure 3a. Na spectra are formed by three components at ~0, -10 and -19 ppm that have been assigned, in agreement with a previous work (Laperche et al., 1990), to Na^+ ions in two-layers, one-layer and anhydrous phases. In saponites with $x_t < 0.3$, the main line corresponds to the two-layer hydrate; however, in micas, with $x_t > 0.3$, the main components correspond to one-layer or anhydrous phases. As x_t increases the amount of anhydrous phase increases, becoming the unique phase for $x_t > 0.38$ samples. In dried samples, ^{23}Na MAS-NMR spectra are formed by a broad asymmetric band that shifted from -22.4 to -11.6 ppm as tetrahedral Al content increases. In micas, the linewidth decreased considerably with respect to saponite samples (Figure 3b).

^{27}Al MAS-NMR spectra of analyzed samples are given in Figure 4. In agreement with proposed compositional schemes, spectra of Na-saponites contain one tetrahedral component whose position changes slightly from 65.2 to 63.7 ppm (Figure 4a). In samples with x_t =0.21 and 0.25, tetrahedral components broaden and become asymmetric. In dried saponites, tetrahedral lines broaden considerably and shift towards more negative values (Figure 4b). These observations are mainly due to second order quadrupolar effects associated with the asymmetric arrangement of Na^+ cations around Al atoms. The Na-micas spectra exhibit two complex components at ~ 70 and 10 ppm, ascribed to tetra- and octahedral aluminium. In these samples, tetrahedral Al components narrow and move towards higher chemical shift values as a consequence of the partial decrement of quadrupole interactions in Al-rich members (Figure 4b). In micas, two detected octahedral components can be ascribed: 1) to the location of Al at M1 and M2 sites, or 2) to the formation of $R^{2+}R^{2+}R^{3+}$ and $R^{3+}R^{3+}$vac associations in octahedral sheets. An estimation of tetra and octahedral aluminium has been performed from central components. In general, deduced values agree with mineralogical formula, however, some overestimation of tetrahedral Al is produced in micas (see Table 2b).

^{29}Si MAS-NMR spectra of analyzed phyllosilicates are formed by four $Q^3(nAl)$ components associated with Si_3, Si_2Al, $SiAl_2$ and Al_3 environments (denoted by 0, 1, 2 and 3 in Figure 5). In hydrated Na-saponites (two-layer hydrates), three narrow components ascribed to the first three environments have been detected, with relative intensities changing according to chemical composition of samples. The position of each component shifts towards more positive values as tetrahedral Al increases (Figure 5a). In dehydrated saponites, bands broaden considerably and two peaks were resolved (Figure 5b). In order to analyze quantitatively NMR spectra of samples, each environment was considered to be formed by two components with similar linewidths. In dried samples, linewidths turned out to be considerably higher (FWHM = 3-3.5 ppm) than those observed in hydrated ones (FWHM = 2 ppm). The positions and intensities of resolved components are given in Table 2a.

In the case of dried $Na(Mg_{3-y}Al_y)(Si_{3-y}Al_{1+y})O_{10}(OH)_2$ micas, ^{29}Si MAS-NMR spectra are formed by four mentioned components. As the tetrahedral Al content increases, the intensity of components associated with $SiAl_2$ and Al_3 increase at expenses of Si_2Al and Si_3 environments (Figures 5b). In preiswerkite (Si_2Al_2 composition), the Al_3 environment becomes dominant. In the case of the hydrated Na-mica with x_t = 0.38, formerly known as Na-eastonite, five detected components have been reproduced by considering the spectrum as sum of two phases detected by XRD, the one-layer hydrate and the anhydrous phyllosilicate. The four bands of the hydrated phase are shifted from those of the anhydrous one by 2.5 ppm along the abscissa axis (Figure 5a). When this sample is dried, the spectrum becomes simplified, remaining only the four expected components of anhydrous phases (Figure 5b). Intensities of Si and Al MAS-NMR components are given in Table 2b.

DISCUSSION

Along saponite-mica series, the amount of tetrahedral aluminum per structural formula increases in a continuous way from 0.33 to 2 ($0.08 < x_t < 0.5$). In two

series, charge compensating mechanisms have been investigated: a) in saponites, octahedral composition basically remains Mg_3, and the increasing amount of Al_t is compensated by interlamellar Na^+ cations, b) in Na-micas, the amount of interlamellar cations remains constant, and charge deficits introduced by Al_t are compensated by the partial replacement of Mg by Al in octahedral layers. Both mechanisms have been confirmed by ^{27}Al MAS-NMR spectroscopy, using the same amount of sample in quantitative determinations. In saponites, the amount of the tetrahedral Al (intensity of the ~70 ppm band) increases with Na content; but in micas, the intensity of tetra and octahedral components increase simultaneously; confirming the Al-Tschermak substitutional scheme. The linewidth of the tetrahedral Al NMR component increases with the aluminum content between x_t= 0.12 and 0.25, decreasing again between 0.25 and 0.5. These observations suggest the presence of several tetrahedral configurations (structural disorder) for intermediate compositions. The spectral broadening is more visible in dried saponites, where elimination of sodium mobility increases second order quadrupolar effects.

Under high water vapour pressure (≥ 85 %), three hydration states are recognized in studied phyllosilicates (de la Calle, 1988; Güven, 1988). They can be distinguished by their basal distance d_{001}: (1) two-layer hydrate saponites with $5H_2O$ per Na and $d_{001} \approx 15$ Å, in the compositional range $0.33 < x < 1$; (2) one layer hydrate with $2H_2O$ per Na and $d_{001} \approx 12$ Å, dominant for $x = 1$ saponites and $y < 0.5$ micas, and (3) anhydrous phases, with $d_{001} \approx 10$ Å, typical of micas with high y values. The tetrahedral distortion, described with α angle, increases with the tetrahedral Al content, as a consequence of the tetra- and octahedral layers misfit. In analyzed phyllosilicates, the two-layer hydrate is observed for $\alpha \leq 10^\circ$, the one-layer hydrate is dominant for $10^\circ < \alpha < 16^\circ$, and beyond $\alpha \geq 16^\circ$, only anhydrous phyllosilicates are obtained. According to this, low rotation angles, α, favour the Na^+ hydration; whereas high α values, favour the Na^+ coordination by tetrahedral layer oxygens.

^{23}Na MAS-NMR spectra have been used to follow the hydration of samples. In saponite and mica series, three components have been detected that correspond

to two-layers, one-layer and anhydrous phases. In agreement with X-ray data, NMR spectra of saponites display a single band at ~ 0 ppm, assigned to two-layer hydrates. In micas with intermediate $^{[6]}$Al contents, NMR spectra exhibit two components at ~ -10 and 19 ppm, associated with one-layer and anhydrous phases. In Al-rich micas, like preiswerkite $Na(Mg_2Al)(Si_2Al_2)O_{20}(OH)_2$, only the band ascribed to anhydrous phases was detected. In anhydrous phases, ^{23}Na MAS-NMR spectra display one asymmetric large component near -20 ppm that has been assigned to the existence of Na polyhedra with a higher coordination number. Above $x_t > 0.30$, the linewidth decreases and components shifts towards more positive values, as a consequence of the more regular cation disposition (lower quadrupole interactions).

In phyllosilicates, each tetrahedron shares three oxygens with adjacent tetrahedra to form hexagonal patterns (Figure 1). According to the Loewenstein's rule (Al_t-O-Al_t avoidance), ^{27}Al NMR spectra only display one component ascribed to Al surrounded by 3Si, but ^{29}Si NMR spectra can be formed by four lines ascribed to Si_3, Si_2Al, $SiAl_2$ and Al_3 environments (lines denoted as 0, 1, 2 and 3). The intensity of Si components involving a higher amount of Al, increases with the Al fractional content. In the case of saponites $Na_xMg_3(Si_{4-x}Al_x)O_{10}(OH)_2$, with $0.33 \leq x \leq 1$, spectra are mainly formed by Si_3, Si_2Al and $SiAl_2$ environments, but in the case of $Na(Mg_{3-y}Al_y)(Si_{3-y}Al_{1+y})O_{10}(OH)_2$ micas, with $0 \leq y \leq 1$, spectra are formed by the four components, increasing the intensity of Si_2Al and Al_3 components as the tetrahedral Al content increases..

In preiswerkite $Na(Mg_2Al)(Si_2Al_2)O_{10}(OH)_2$, the ^{29}Si NMR spectrum is formed by an important Al_3 line and a small one due to $SiAl_2$ environments. According to the Loewenstein's rule, the alternation of Si and Al in tetrahedral sheets, should produce the differentiation of two tetrahedral sites. However, the XRD study of a single crystal of preiswerkite (Oberti et al., 1993) showed that a unique site was occupied by Si and Al, (C2/m symmetry). In analyzed preiswerkite, the detection of two components is probably associated with slight deviations from ideal composition. Similar deviations have been deduced for $x_t = 0.44$ sample (see Table1). In order to explain ^{29}Si NMR results, the existence of anti-phase domains could justify the absence of unit cells with two tetrahedral sites.

When the Loewenstein's rule (Al_t-O-Al_t avoidance) is obeyed in tetrahedral sheets of phyllosilicates, it is possible to deduce tetrahedral Si/Al ratios from ^{29}Si MAS-NMR spectra through the expression:

$$Si/Al = \sum_n I_n / (0.33 \sum_n n.I_n) = (1-x_t)/x_t$$

where I_n denotes intensities of Si NMR components associated with nAl.(3-n)Si, environments (Sanz and Serratosa, 1984). From Si/Al ratios, tetrahedral Al fractional contents, x_t, were determined. The x_t values deduced from hydrated and anhydrous phases, are similar and coincide within 5% with nominal compositions, indicating that all samples are on-composition and comply with the Loewenstein's rule (Sanz and Robert, 1992). In analyzed samples, deduced x_t values were compared with nominal tetrahedral Al contents. In general, x_t values deduced from ^{27}Al NMR are slightly higher than deduced from ^{29}Si NMR spectroscopy. indicating that the quantification of Al bands is more difficult when quadrupolar effects are present.

Besides Loewenstein's rule, Si and Al are homogeneously dispersed in the tetrahedral sheets of phyllosilicates (Barron at al., 1985; Herrero et al. 1985, 1989; Circone et al., 1991). This criterium was included in Monte Carlo simulations by imposing that the number of Al in hexagonal rings is close to average values deduced from chemical compositions. The intensities of four detected Si_3, Si_2Al, $SiAl_2$ and Al_3 bands, were calculated on the bases of the HDC (Homogeneous Distribution of Charges) model as a function of x_t values (Herrero et al., 1989). The agreement between experimental and calculated values is remarkable, indicating that a homogeneous dispersion of tetrahedral charges is produced (Sanz and Robert, 1992).

In hydrated saponites, Si NMR components are considerably narrower than in dried samples. This observation suggests that sodium and water motions average the charge seen by different Si tetrahedra, making shifts of components

to depend in a linear way on the interlamellar charge (Sanz et al. 2006). This is favoured by the fact that Na^+ ions are coordinated to six water molecules (two-layer hydrates), which allocates water protons near charge-deficient tetrahedra. In dried samples, elimination of adsorbed water reduces sodium mobility, making less probable Na^+ exchange processes between structural sites. The increasing residence time of Na^+ cations near tetrahedral charge deficits, favours quadrupole and dipolar interactions with tetrahedral Al.

In hydrated micas, the scene is different from saponites. In the hydrated sample with x_t = 0.38, i.e. Na-eastonite, five components are detected in ^{29}Si MAS-NMR spectra; and XRD pattern show the mixture of one-layer hydrate and anhydrous phase. In agreement with this observation, ^{29}Si NMR spectrum is formed by the superposition of two similar four-component patterns. The pattern assigned to the anhydrous phase was shifted by 2.5 ppm with respect to that of the hydrated phase. The dehydration produces the elimination of the NMR pattern associated with one-layer hydrate, producing a considerable simplification of the ^{29}Si NMR spectrum (Figure 5b).

In dried saponites, the elimination of adsorbed water broadens considerably Si NMR bands, favouring the components splitting. Taking into account the different influence of octahedral and interlamellar charge on ^{29}Si chemical shift values of phyllosilicates 2:1 (Sanz et al., 2006), two resolved bands have been ascribed to differences in the number of Na that surround a particular tetrahedron. In agreement with this fact, the variation observed on chemical shift values of Si_3, Si_2Al, $SiAl_2$ and Al_3 components (Figure 6) is higher in saponites (layer charge 0.33-1) than in Na-micas, where the amount of interlamellar sodium is constant (layer charge 1). The observed variation of ^{29}Si chemical shifts of hydrated samples results from averaging Si NMR components with different number of Na, from 0 to 3, in three adjacent hexagonal rings.

In anhydrous micas, Na^+ cations are engaged in two hexagonal rings of contiguous layers, shifted each other in [-1 0 0], [1 1 0] and [-1 1 0] directions (Rausell-Colom et al., 1980; Kogure et al, 2004, 2005). The layer shift minimizes electrostatic repulsions between contiguous layers and favours the hydration of

micas. The elimination of water molecules increase the amount of Na^+ cations that are placed in three hexagonal rings that surrounds a particular tetrahedron (Figure 6). This elimination is responsible for the discontinuity observed at x_t~0.38 in chemical shifts of four detected components of micas (Figure 6).

In agreement with HDC model, hexagonal rings with 0 and 1 Al should be favoured in dehydrated $x_t < 0.17$ phyllosilicates, those with 1 and 2 Al in samples with $0.17 \leq x_t \leq 0.33$, and those with 2 and 3 Al in samples in the $0.33 \leq x_t \leq 0.5$ range. An estimation of the average amount of Na^+ cations that surround a particular tetrahedron is given as a function of the tetrahedral Al content, x_t, in Figure 7a. In dried saponites, NMR peaks split into two components: in samples with $x_t < 0.09$, detected components should correspond to Si without or near 1 Na. In the range of x_t = 0.09-0.17, two components, labelled A and B in Figure 3b, should correspond to Si surrounded by 1Al and 2Al; the relative intensity of the B component increasing at expenses of the A component when tetrahedral Al increases. Between x_t = 0.17 and 0.25 two detected components should correspond to Si surrounded by 2 and 3 Na. In samples with $x_t > 0.25$, all hexagonal rings are occupied by sodium and each tetrahedron is surrounded by 3Na. The sample drying, affects considerably ^{23}Na and ^{27}Al and NMR spectra, producing the quadrupolar broadening of NMR components by anisotropic arrangement of Na^+ and Al^{3+} cations (Rausell-Colom et al., 1980). In the case of tetrahedral Al NMR signals, the presence of second order quadrupolar effects prevented the resolution of interlamellar environments. In micas with $x_t > 0.33$, Na and Al distribution become regular, decreasing the linewidth of ^{23}Na and ^{27}Al NMR signals.

In the case of the dried Na-phlogopite, x_t = 0.25, HDC simulations show that the local compensation of Na^+ cations was achieved by the superposition of 1 Al and 2 Al hexagonal rings of adjacent layers (Figure 7b). In this phase, all hexagonal rings are occupied by Na, and each tetrahedron is surrounded by 3 Na^+ cations. In micas with $x_t > 0.25$, increasing amounts of tetrahedral Al are compensated by octahedral Al. In the case of the preswerkite (Si_2Al_2 composition), the compliance of the Loewenstein's rule should produce the strict alternation of Si and Al in hexagonal rings (Si tetrahedra surrounded by 3Al and Al surrounded by 3Si), that

was not confirmed. Observed differences have been ascribed to slight deviations on the composition of the sample (x_t = 0.47 versus to 0.50).

In anhydrous micas, the increase of tetrahedral Al produces the ditrigonal distortion of hexagonal rings (Figure 1), that should shift Si NMR components towards more positive values (Sanz and Robert, 1992). However, estimated α values vary from 4° to ≈ 10º in saponites and from ≈ 10 to ≈ 19° in Na-micas. This observation indicates that the variation of chemical shift is not strictly proportional to α values, and other structural factors affect chemical shift values. Based on this fact, changes observed in chemical shift values of Si_3, Si_2Al, $SiAl_2$ and Al_3 bands have been ascribed to changes in the interlayer charge (Sanz et al, 2006b). The elimination of adsorbed water cancels the chemical shifts averaging, allowing the resolution of additional environments. Similar facts should also be produced in zeolites; however, these observations have not been reported.

IMPLICATIONS

Non-periodic arrangements of atoms are difficult to investigate with diffraction techniques because long range order (LRO) is required. In these cases, short (SRO) or medium (MRO) range associations can be studied by spectroscopic methods. In this work, cation distribution and interlamellar mobility have been investigated by NMR spectroscopy in sodium phyllosilicates.

In hydrous $(Na,Ca)_xSi_{3-y}Al_y(Al,Mg,vac)_3O_{10}OH_2.nH_2O$ phyllosilicates, physico-chemical properties depend on the location and distribution of the silicate charge. In reported classifications, it has been considered relevant to differentiate dioctahedral ($R^{3+}R^{3+}vac$) and trioctahedral ($R^{2+}R^{2+}R^{2+}$) phases. According to this, montmorillonites (octahedral charge), beidellites (tetrahedral charge) and vermiculites (tetra and octahedral charge) have been differentiated in dioctahedral phyllosilicates. In trioctahedral samples, hectorites (octahedral charge), saponites (tetrahedral charge) and vermiculites (tetra and octahedral charge) have been considered separately (S. Caillère et al., 1982). In a more recent classification, N. Güven has considered that the nature of compensating

cations affect hydration, sweeling and layer stacking of different phyllosilicates (N. Güven, 1988). In this work, only sodium phyllosilicates have been considered. The preparation of sodium synthetic samples has permitted a separated analysis of cation substitution schemes in saponites and hydrated micas. In this series, tetrahedral charge deficits, generated by Al for Si substitution, are compensated by interlamellar Na in smectites and by octahedral Al in micas. In tetrahedral layers, Al fulfils the Loewenstein's rule (Al-O-Al associations) and the homogeneous dispersion of charges. Similar distribution features where also identified in tectosilicates (Dempsey et al, 1969). The present study should be extended to trioctahedral hectorites where the silicate charge is located at octahedral layers of phyllosilicates. A similar study should be performed in dioctahedral phyllosilicates, where distribution of octahedral charges comply other crystallo-chemical requirements.

In agreement with results described here, the sodium coordination depends through the tetrahedral tilting on the aluminium content. In saponites, small tetrahedral tiltings favour the sodium hydration, but in micas, anhydrous phases are favoured for bigger tiltings. In analyzed samples, the Na coordination results from the competition of water and basal oxygen bonding of interlamellar cations. The comparison of hydrated and anhydrous phases illustrates the presence of sodium and water motional effects. The arrangement and mobility of water have special relevance in hydration and transport properties (Hougardy et al., 1976, Fripiat,et al., 1984). These studies have special relevance in immobilization of contaminant cations (Laperche et al., 1990).

Information deduced here has special relevance in mineralogy and geochemistry of hydrous phyllosilicates. The progressive modification of the phyllosilicate network detected along the series questions the existence of compositional limits for the saponites-hydrated micas classification (de la Calle and Suquet, 1988). On the other hand, the analysis of heterogeneous distributions of charges could be used to understand the origin of interstratified phyllosilicates (Altaner and Ylagan, 1997). Taking into account that long range arrangements detected by X-ray diffraction (LRO structures) are a consequence of short-range interactions

(SRO), diffraction and spectroscopic methods should be used in phyllosilicates classification.

ACKNOWLEDGEMENTS

The authors wish to dedicate this work to the memory of Prof. José Maria Serratosa who intensively promoted NMR studies addressed to improve the crystal-chemical knowledge of clay minerals. He passed away on November 22, 2012.

REFERENCES

Altaner, S.P. and Ylagan, R.E. (1997) Comparison of structural models of mixed layer illite/smectite and reaction mechanisms of smectite illitization. Clays and Clay Minerals, 45, 57-533..

Bailey, S.W. (1984) Crystal chemistry of the true micas. In: Reviews in Mineralogy, Vol. 13, S.W Bailey Ed., Mineralogical Society of America, 13-60.

Barron, P.F., Slade, P. and Frost R.L. (1985) Ordering of aluminium in tetrahedral sites in mixed layer 2:1 phyllosilicates by solid-state high-resolution NMR. Journal of Physical Chemistry, 89, 3880-3885.

Caillère, S., Hénin, S., Rautureau, M. (1982) Minéralogie des argiles. 2. Classification et Nomenclature. 2 edition.. Actualités scientifiques et agronomiques, 9, INRA et Masson, Paris.

Carman, J.H. (1974) Synthetic sodium phlogopite and its two hydrates: stabilities, properties and mineralogic implications. American Mineralogist, 59, 261-273.

Circone, S., Navrotsky, A., Kirkpatrick, R.J., and Graham, C.M. (1991) Substitution of $^{[6,4]}$Al in phlogopite: Mica characterization, unit cell variation, ^{27}Al

and ^{29}Si MAS-NMR spectroscopy, and Al-Si distribution in the tetrahedral sheet. American Mineralogist, 76, 1485-1501.

De la Calle, C., and Suquet, H. (1988) Vermiculites. Hydrous Phyllosilicates (exclusive of micas). In: Reviews in Mineralogy, Vol. 19, S.W. Bailey Ed., Mineralogical Society of America, 455-496.

Dempsey, E., Kuhl, G.H., and Olson, D.H. (1969) Variation of the lattice parameter with aluminum content in synthetic sodium faujasites. Evidence for ordering of the framework ions. Journal of Physical Chemistry, 73, 387–390.

Donnay, G., Morimoto, N., Takeda H., and Donnay, J.D.H. (1964a) Trioctahedral one-layer micas. I. Crystal structure of a synthetic iron mica. Acta Crystallographica, 17, 1369-1373.

Donnay, G., Donnay, J.D.H., and Takeda, H. (1964b) Trioctahedral one-layer micas. II. Prediction of the structure from composition and cell dimensions. Acta Crystallographica, 17, 1374-1381.

Fripiat, J., Letellier, M. and Levitz, P. (1984) Interaction of water with clay surfaces. Phil. Trans. Royal Soc. London, 311, 287-299.

Güven, N. (1988) Smectites. Hydrous Phyllosilicates (exclusive of micas). In: Reviews in Mineralogy, Vol. 19, S.W. Bailey Ed., Mineralogical Society of America, 497-560.

Hamilton, D.L., and Henderson, C.M.B. (1968) The preparation of silicate compositions by a gelling method. Mineralogical Magazine, 35, 832-838.

Hazen, M.R., and Burnham, C.W. (1973) The crystal structure of one-layer phlogopite and annite. American Mineralogist, 58, 889-900.

Herrero, C.P., Sanz, J., and Serratosa, J.M (1985) Tetrahedral cation ordering in layer silicates by ^{29}Si NMR spectroscopy. Solid State Communications, 53, 151-154.

Herrero, C.P., Sanz, J., and Serratosa, J.M. (1989) Dispersion of charge deficits in the tetrahedral sheet of phyllosilicates. Analysis from ^{29}Si NMR spectra. Journal of Physical Chemistry, 93, 4311-4315

Hougardy, J., Serratosa, J.M., Stone, W., and Van Olphen, H. (1970) Interlayer Water in Vermiculite: Thermodynamic Properties, Packing Density, Nuclear Pulse Resonance, and Infra-Red Absorption. Special Discussions of The Faraday Society, 1, 187-193.

Hougardy, J., Stone, W.E.E., and Fripiat, J.J. (1976) NMR study of adsorbed water. I. Molecular orientation and protonic motions in the two-layer hydrate of a Na-vermiculite, Journal of Chemical Physics, 64, 168-179.

Kogure, T., Banno, Y., Miyawaki, R. (2004) Interlayer structure in aspidolite, the Na analogue of phlogopite, European Journal of Mineralogy, 16, 891-897.

Kogure, T., Miyawaki, R., Banno, Y. (2005) The true structure of wonesite, an interlayerdeficit trioctahedral sodium mica. American Mineralogist, 90, 725-731. .

Laperche, V., Lambert, J.F., Prost, R., and Fripiat, J.J. (1990) High-resolution solid state NMR of exchangeable cations in the interlayer surface of a swelling mica: ^{23}Na, ^{111}Cd and ^{133}Cs vermiculites. Journal of Physical Chemistry, 94, 8821-8831.

Liu Xiang, Feng (1989) Signification pétrogénétique des micas trioctaédriques sodiques. Etude expérimentale et cristallochimique dans le système Na_2O-K_2O-MgO-Al_2O_3-SiO_2-H_2O-(D_2O-TiO_2-HF). Thèse Université d'Orléans.

Massiot, D. (1993) WINFIT, Bruker-Franzen Analytik GmbH, Bremen, Germany.

Oberti, R., Ungaretti, L., Tilli, A., Smith, D.C., and Robert, J.L. (1993) The crystal structure of preswerkite. American Mineralogist, 78, 1290-1298.

Rausell-Colom, J.A., Fernandez, M., Serratosa, J.M., Alcover, J.F., and Gatineau, L. (1980) Organisation de l'espace interlamellaire dans les vermiculites monocouches et anhydres. Clay Minerals, 15, 37-57.

Rieder, M., Cavazzini, G., D'Yakonov Yu., S., Koval, P.V., Müller, G., Neiva, A.M. R., Sassi, F.P., Takeda, H., Weiss, Z., Frank-Kamenetskii, V.A., Gottardi, G., Guggenheim, S., Radoslovich, E.W., Robert, J.L., and Wones, D.R. (1999) Nomenclature of the Micas. Mineralogical Magazine, 63, 267-279.

Sanz, J., and Serratosa, J.M. (1984) ^{29}Si and ^{27}Al high-resolution MAS-NMR spectra of phyllosilicates. Journal of American Chemical Society, 106, 4790-4793.

Sanz, J., and Robert, J.L. (1992) Influence of structural factors on ^{29}Si and ^{27}Al NMR chemical shifts of phyllosilicates 2:1. Physics and Chemistry of Minerals, 19, 39-45.

Sanz, J., Robert, J.L., Diaz, M., and Sobrados, I. (2006a) Influence of charge location on ^{29}Si NMR chemical shift of 2:1 phyllosilicates. American Mineralogist, 91, 544-550.

Sanz, J., Herrero, C.P., and Serratosa, J.M. (2006b) Arrangement and mobility of water in vermiculite hydrates followed by ^{1}H NMR spectroscopy. Journal of Physical. Chemistry., 110, 7813-7819.

FIGURE CAPTIONS.

Figure 1. Structure of dried phyllosilicates, illustrating the tetrahedal distortion described by Donnay et al. (1964b).

635 Figure 2, Disposition of Na cations in two-layer, one-layer and anhydrous phases
636 proposed by Hougardy et al. (1976), de la Calle et al. (1988) and Rausell-Colom
637 et al. (1980).
638
639 Figure 3. ^{23}Na MAS-NMR spectra of wet (a) and dried (b) Na phyllosilicates,
640 where Na components ascribed to two-layer, one-layer and anhydrous phases
641 are resolved.
642
643 Figure 4. ^{27}Al MAS-NMR spectra of wet (a) and dried (b) Na phyllosilicates,
644 where tetrahedral and octahedral Al bands are detected.
645
646 Figure 5. ^{29}Si MAS-NMR spectra of wet (a) and dried (b) Na phyllosilicates, where
647 Si_3, Si_2Al, $SiAl_2$ and Al_3 environments are denoted by integer numbers 0, 1, 2 and
648 3. Bands denoted A and B in deconvolutions are associated with differences on
649 the interlayer environment (see text). Details on spectral deconvolution are given
650 in the experimental section.
651
652 Figure 6. Dependence of ^{29}Si chemical shifts on the tetrahedral Al fractional
653 content, x_t, of phyllosilicates. In this plot, different slopes were detected for
654 two-layer (HII), one-layer (HI) and anhydrous phases (Sanz et al., 2006b).
655
656 Figure 7. a) Relative proportion of Si tetrahedra surrounded by hexagonal rings
657 with 0, 1, 2 and 3 Na in dried phyllosilicates. b) Schematic view of two tetrahedral
658 sheets located at both sides of Na cations in $x_t = 0.25$ micas. In this figure, Al
659 tetrahedra of adjacent layers are denoted with different colours.
660

Table 1 – Tetrahedral composition; x_t, deduced from chemical analyses and Si MAS-NMR spectroscopy; d_t, (Å), the average T-O distance in tetrahedra, and α(°), the ditrigonal angle of tetrahedra deduced with Donnay et al. expressions (1964b). Errors in x_t values are lower than 0.01.

Tetrahedral composition	x_t	$x_{t\ (NMR)}$	d_t (Å)	α(°)
$Si_{3.52}Al_{0.48.}$	0.12	0.13	1.628	4.1
$Si_{3.36}Al_{0.64}$	0.16	0.16	1,634	5.2
$Si_{3.16}Al_{0.84}$	0.21	0.20	1.642	7.6
Si_3Al	0.25	0.25	1.649	10.1
$Si_{2.8}Al_{1.2}$	0.30	0.29	1.657	11.4
$Si_{2.5}Al_{1.5}$	0.38	0.38	1.670	15.5
$Si_{2.25}Al_{1.75}$	0.44	0.41	1.680	17.2
Si_2Al_2	0.50	0.47	1.689	18.9

TABLE 2a. ^{29}Si MAS-NMR parameters (chemical shifts and intensities) deduced from the study of Na saponites and Na micas.

Errors in chemical shifts are 0.1 ppm and in intensities 3 %.

Wet samples	Si(3Si)				Si(2SiAl)				Si(Si2Al)				Si(3Al)			
	ppm	%	ppm	%	ppm	%	ppm	%	ppm	%	ppm	%	ppm	%	ppm	%
$Si_{3.52}Al_{0.48}$	-96.2	70	-		-91.4	30	-		-		-		-		-	
$Si_{3.36}Al_{0.64}$	-95.1	52	-		-90.4	46	-		-85.9	2	-		-		-	
$Si_{3.16}Al_{0.84}$	-93.8	32	-		-89.3	59	-		-85.2	9	-		-		-	
$Si_{2.8}Al_{1.2}$	-92.4	9	-90.9	5	-88.0	34	-86.4	17	-84.0	19	-82.0	12	-80.2	2	-77.8	2
$Si_{2.5}Al_{1.5}$	-91.4	4	-88.1	6	-87.5	16	-84.9	16	-83.6	19	-81.4	25	-80.0	4	-77.9	10
$Si_{2.25}Al_{1.75}$	-		-87.1	6	-		-84.0	21	-		-80.5	41	-		-77.2	32
Si_2Al_2	-		-		-		-		-		-80.5	31	-		-77.1	69

Dry samples	Si(3Si)				Si(2SiAl)				Si(Si2Al)				Si(3Al)			
	A		B		A		B		A		B		A		B	
	ppm	%	ppm	%	ppm	%	ppm	%	ppm	%	ppm	%	ppm	%	ppm	%
$Si_{3.52}Al_{0.48}$	-97.3	53	-94.2	21	-90.6	26							-		-	
$Si_{3.36}Al_{0.64}$	-97.1	30	-94.1	24	-90.9	25	-88.8	18	-85.3	2	-83.7	1	-		-	
$Si_{3.16}Al_{0.84}$	-95.3	13	-92.8	21	-89.1	33	-87.2	21	-84.1	7	-81.8	5	-		-	
$Si_{2.8}Al_{1.2}$	-		-91.0	17	-		-86.4	53	-		-81.9	30	-		-	
$Si_{2.5}Al_{1.5}$	-		-88.7	11	-		-85.1	33	-		-81.2	39	-		-77.4	17
$Si_{2.25}Al_{1.75}$	-		-87.1	6	-		-84.0	21	-		-80.5	40	-		-77.2	33
Si_2Al_2	-		-		-		-		-		-80.5	30	-		-77.1	70

TABLE 2b. ^{27}Al MAS-NMR parameters (positions and intensities) deduced from the study of Na saponites and Na micas.

Errors in positions are 0.2 ppm and in intensities 3 %.

Wet samples	Si (NMR)	Al (NMR)			
	Al_t	Al_t		Al_o	
	%	ppm	%	ppm	%
$Na_{0.48}Si_{3.52}Al_{0.48}Mg_3O_{10}(OH)_2$	100	65.2	98	9.0/0.1	2
$Na_{0.64}Si_{3.36}Al_{0.64}Mg_3O_{10}(OH)_2$	100	64.5	97	8.5/0.1	3
$Na_{0.84}Si_{3.16}Al_{0.84}Mg_3O_{10}(OH)_2$	100	63.7	97	8.5/0.1	3
$NaSi_{2.8}Al_{1.2}Mg_{2.8}Al_{0.2}O_{10}(OH)_2$	86.0	64.2	98	8.4/0.1	2
$NaSi_{2.5}Al_{1.5}Mg_{2.5}Al_{0.5}O_{10}(OH)_2$	75.0	68.7	81	8.5/0.1	19
$NaSi_{2.25}Al_{1.75}Mg_{2.25}Al_{0.75}Mg_3O_{10}(OH)_2$	70.0	70.8	78	8.7/0.1	22
$NaSi_2Al_2Mg_2AlMg_3O_{10}(OH)_2$	66.7	71.0	71	9.3/0.1	29
Dry samples	Si (NMR)	Al (NMR)			
	Al_t	Al_t		Al_o	
	%	ppm	%	ppm	%
$Na_{0.48}Si_{3.52}Al_{0.48}Mg_3O_{10}(OH)_2$	100	59.9	99	9.0	1
$Na_{0.64}Si_{3.36}Al_{0.64}Mg_3O_{10}(OH)_2$	100	64.4	98	9.5/0.1	2
$Na_{0.84}Si_{3.16}Al_{0.84}Mg_3O_{10}(OH)_2$	100	64.0	98	9.5/0.1	2
$NaSi_{2.8}Al_{1.2}Mg_{2.8}Al_{0.2}O_{10}(OH)_2$	86.0	65.0	97	9.5/0.1	3
$NaSi_{2.5}Al_{1.5}Mg_{2.5}Al_{0.5}O_{10}(OH)_2$	75.0	68.7	81	8.5/0.1	19
$NaSi_{2.25}Al_{1.75}Mg_{2.25}Al_{0.75}Mg_3O_{10}(OH)_2$	70.0	70.8	78	8.7/0.1	22
$NaSi_2Al_2Mg_2AlMg_3O_{10}(OH)_2$	66.7	71.0	70	9.3/0.1	30

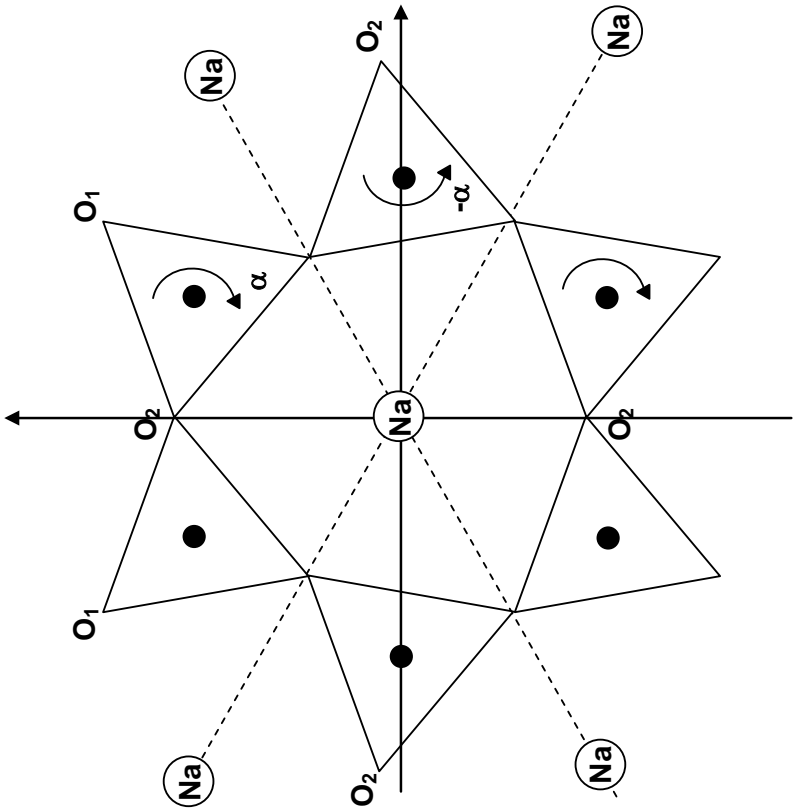

Figure 1. Structure of dried phyllosilicates, illustrating the tetrahedal distortion described by Donnay et al. (1964b).

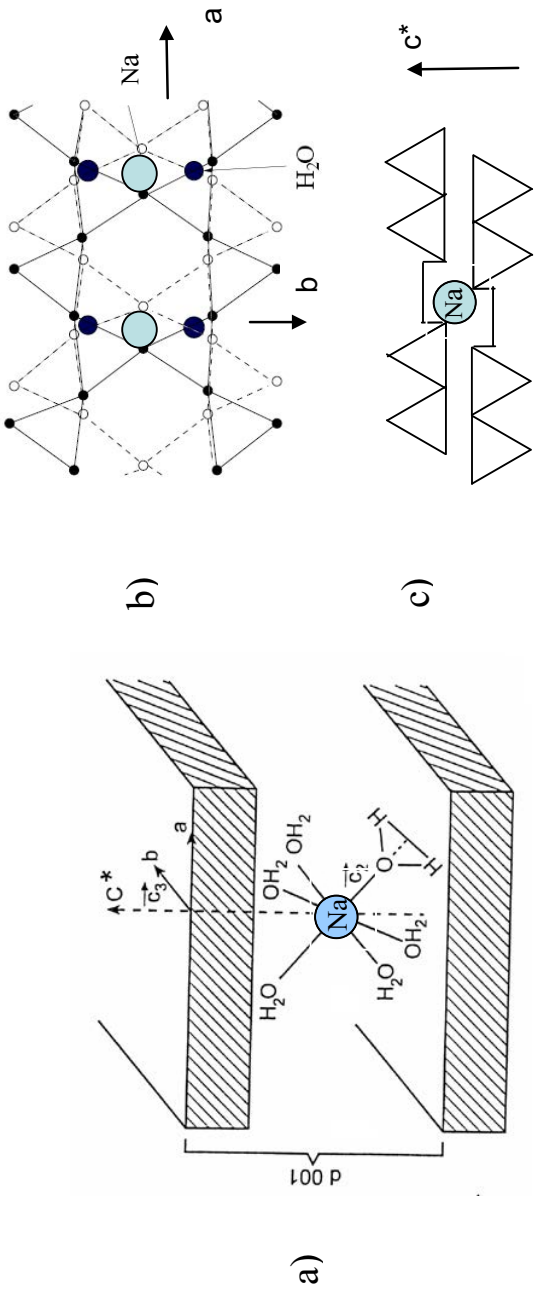

Figure 2. Disposition of Na cations in: a) two-layer, b) one-layer and c) anhydrous phases proposed by Hougardy et al.(1976), de la Calle et al. (1988) and Rausell-Colom et al (1980).

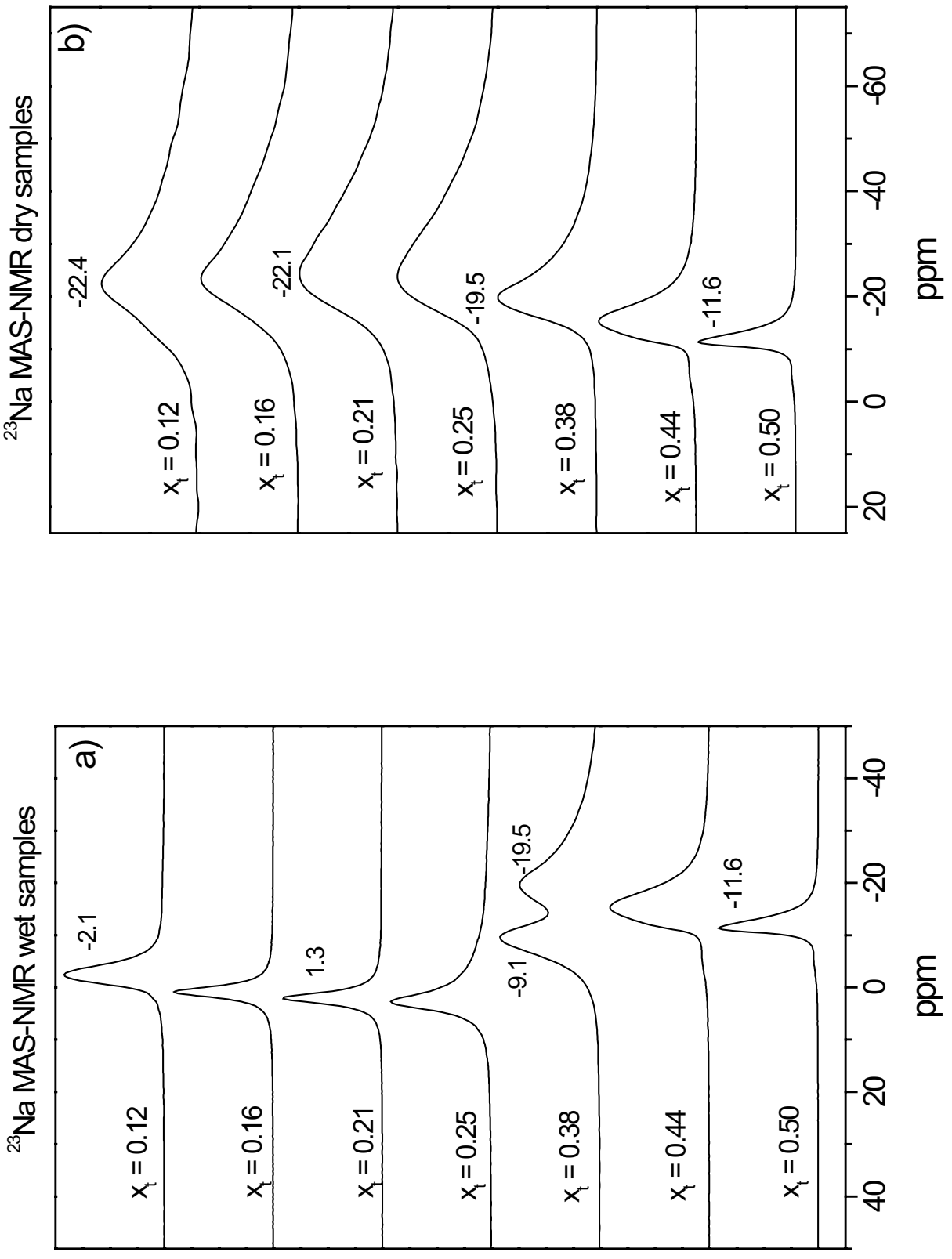

Figure 3. ^{23}Na MAS-NMR spectra of wet (a) and dried (b) Na phyllosilicates, where Na components ascribed to two-layer, one-layer and anhydrous phases are resolved.

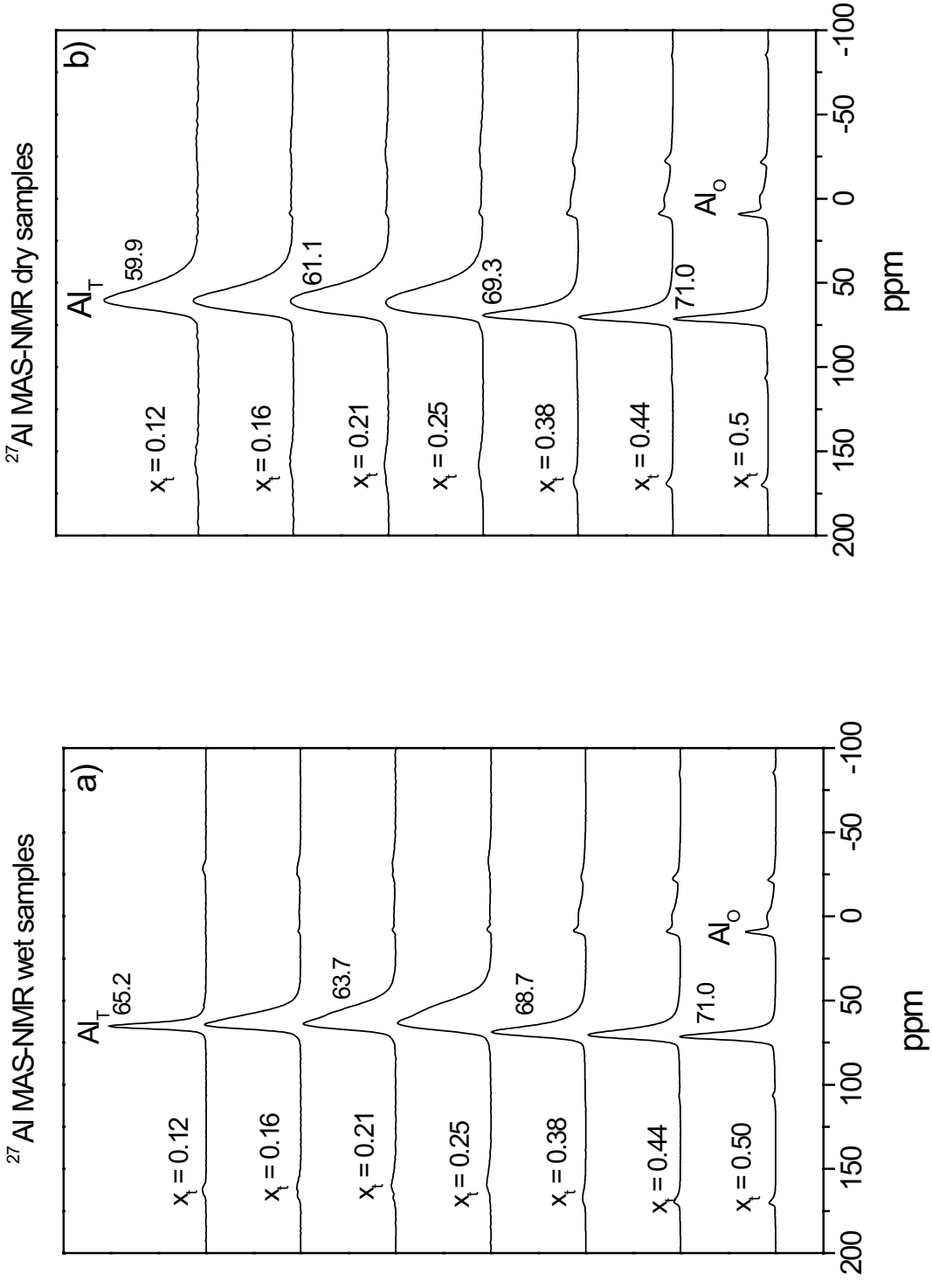

Figure 4. ^{27}Al MAS-NMR spectra of wet (a) and dried (b) Na phyllosilicates, where tetrahedral and octahedral Al bands are detected.

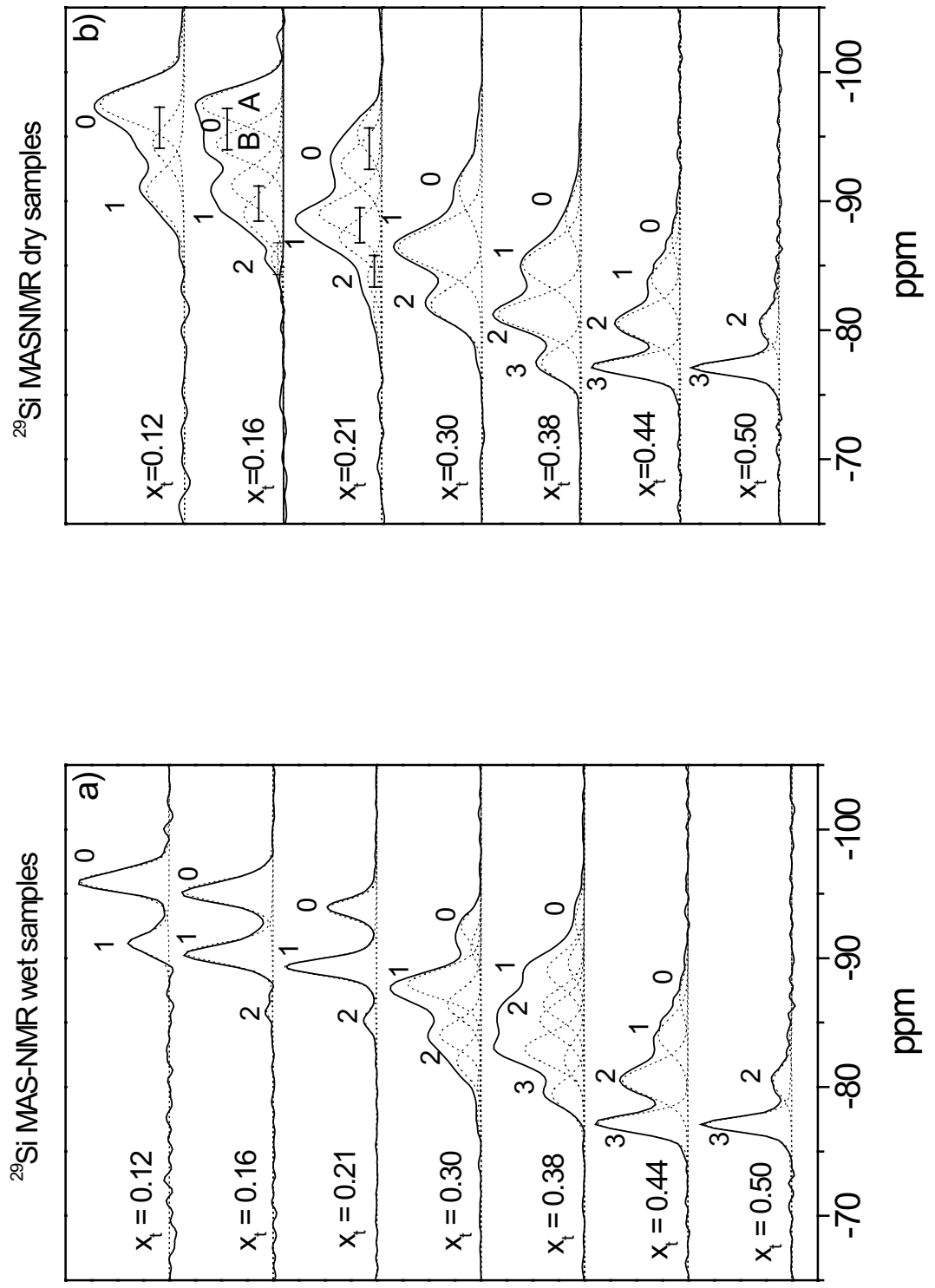

Figure 5. ^{29}Si MAS-NMR spectra of wet (a) and dried (b) Na phyllosilicates, where Si_3, Si_2Al, $SiAl_2$ and Al_3 environments are denoted by integer numbers 0, 1, 2 and 3. Bands denoted A and B in deconvolutions are associated with differences on the interlayer environment (see text). Details on spectral deconvolution are given in the experimental section.

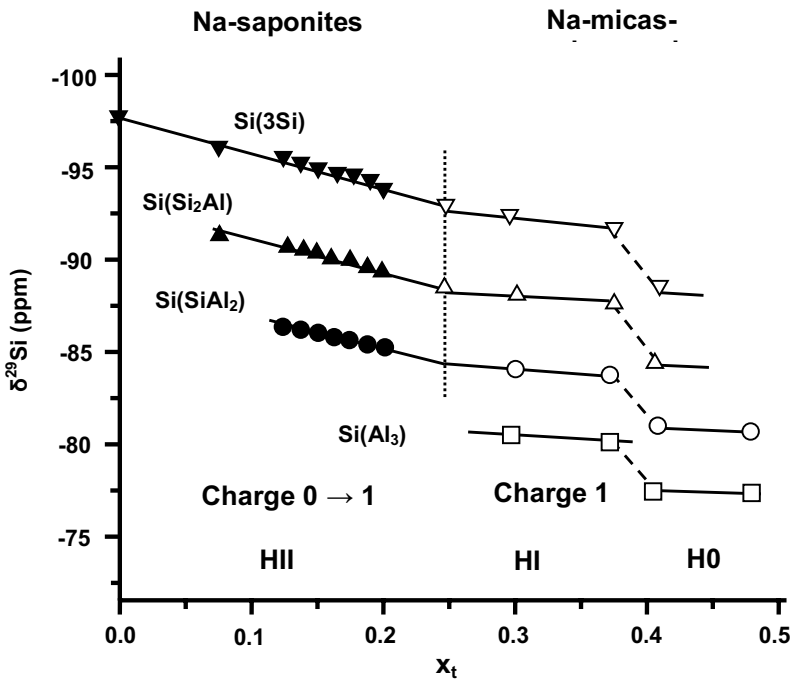

Figure 6. Dependence of ^{29}Si chemical shifts on the tetrahedral Al fractional content, x_t, of phyllosilicates. In this plot, different slopes were detected for two-layer (HII), one-layer (HI) and anhydrous phases (Sanz et al., 2006b)

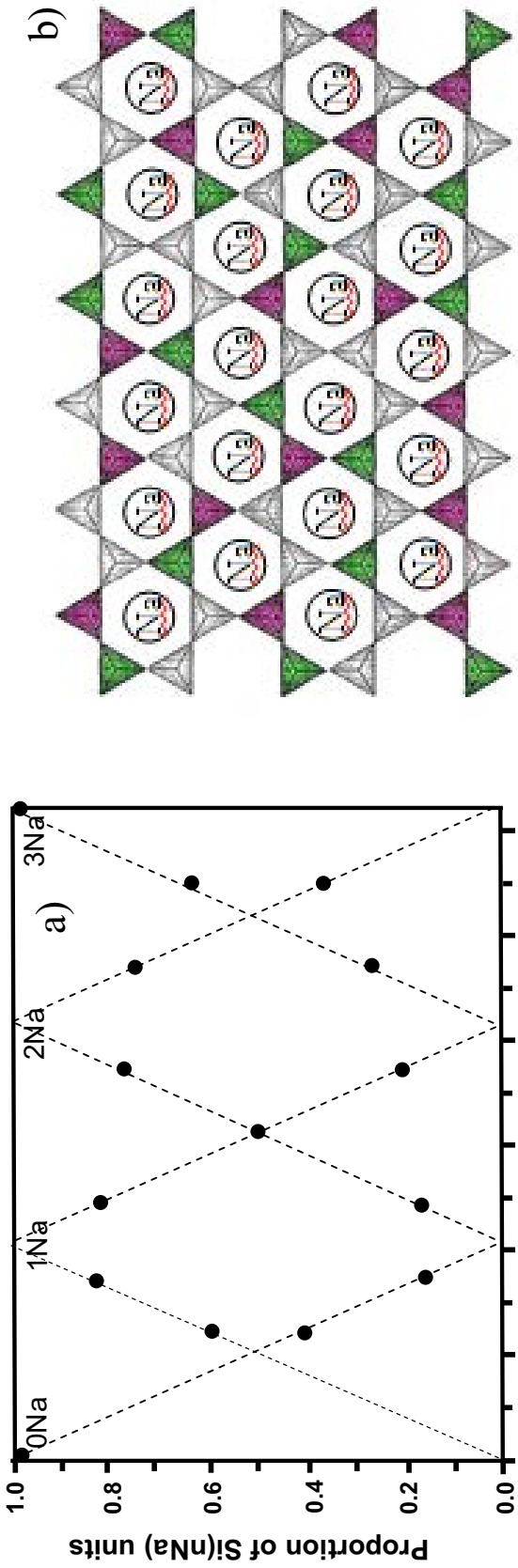

b)

a)

Figure 7. a) Relative proportion of Si tetrahedra surrounded by hexagonal rings with 0, 1, 2 and 3 Na in dried phyllosilicates. b) Schematic view of two tetrahedral sheets located at both sides of Na cations in x_t = 0.25 micas. In this figure, Al tetrahedra of adjacent layers are denoted with different colours.